Solar Energy Materials 13 (1986) 373–384
North-Holland, Amsterdam

PHOTOVOLTAIC PROPERTIES OF AMORPHOUS SILICON PRODUCED BY REACTIVE SPUTTERING

T.D. MOUSTAKAS

Corporate Research Laboratory, Exxon Research and Engineering Company, Annandale, New Jersey 08801, USA

Received 25 October 1985; in revised form 2 January 1986

This paper reviews the photovoltaic properties of amorphous silicon produced by RF diode reactive sputtering. It is divided into three sections. The first part deals with the properties of the intrinsic films. The importance of structural and compositional inhomogeneities, and the role of hydrogen and trace impurities in defining the optoelectronic properties of the material are discussed. The second part deals with the properties of the doped films produced either by gas phase doping or by sputtering from doped targets. Comparison is drawn between totally amorphous and partially crystallized doped films and the superiority of the latter for photovoltaic applications is stressed. Finally, the third section deals with device studies. Solar cells, having the configuration substrate/nip/ITO, generate external currents of 13 mA/cm^2 and open circuit voltages of between 0.85 to 0.95 V. The efficiency of these devices, 5.5%, is limited by the low FF, typically less than 50%. Tandem solar cell structures, having the configuration substrate/nip–nip/ITO, produce an open circuit voltage of 1.8 V. Methods to improve the FF and the J_{sc} through the implementation of amorphous silicon carbide p-type contacts and light trapping techniques are discussed.

1. Introduction

Hydrogenated amorphous silicon can be prepared either by chemical or physical methods of film deposition. In the first class the precursor materials are different forms of silanes, which are decomposed by techniques such as glow discharge decomposition, thermal pyrolysis and photodecomposition. Physical methods include various forms of reactive sputtering (diode, magnetron and ion beam) and reactive evaporation. The kinetics of film growth in these various techniques is not well understood yet. One distinct difference between the chemical and physical methods is that in the first class hydrogen elimination processes are dominant [1], while in the second hydrogen incorporation processes are dominant [2]. Although the mechanisms of growth are different, structural studies of films produced by the various techniques show that the films can be made to have similar short range order, microstructure, and hydrogen bonding configuration.

In this paper we discuss the photovoltaic properties of hydrogenated amorphous silicon produced by reactive RF diode sputtering. We show that the properties of the intrinsic films depend sensitively on structural and compositional inhomogeneities, amount of hydrogen in the films, trace impurity doping and compensation. The properties of doped films, produced either by gas phase doping or by sputtering

from heavily doped targets, are discussed. The merits of partially crystallized films for p and n contacts in photovoltaic devices are demonstrated. Finally, the fabrication methods and performance of various solar cell structures are presented and factors which limit their performance are discussed.

2. Experimental methods

The films and the solar cell structures were deposited in an RF diode sputtering system employing a single deposition chamber. The system was pumped by a combination of turbomolecular and mechanical pumps to a total leak rate of $1-2 \times 10^{-5}$ Torr l s^{-1}, with H_2O being the principal impurity. The total pressure of argon and hydrogen was monitored with a capacitance manometer and the partial pressure of the two gases were measured with a differentially pumped mass spectrometer.

The decomposition chamber has stainless steel walls, held at ground potential, three cathode assemblies and one rotating anode assembly. The three cathode assemblies are furnished with an intrinsic, a boron doped and a phosphorus doped silicon targets. The intrinsic target is 5–9's pure polycrystalline disc. The boron doped target was fabricated by hot pressing fine powders (5–10 μm) of 97 at% Si and 3 at% B. The phosphorus doped target is a single crystal disc containing 200 ppm of phosphorus. All targets, 5″ in diameter and 1/4″ thick, are watercooled and supplied with an RF power at a frequency 13.56 MHz. The anode assembly, 26″ in diameter, is held 2″ below the targets and can be electrically grounded, floated or supplied with RF or DC electrical bias. The substrates are fastened with stainless steel frame and molybdenum springs on the top of the anode assembly and heated radiatively.

Intrinsic films were produced with the substrate temperature, target and substrate voltages, argon and hydrogen partial pressures, and trace impurities as variables. The photovoltaic properties of these films were investigated with Pt-Schottky barrier structures.

Doped films were produced either by gas phase doping (sputtering from the intrinsic target in a mixture of argon, hydrogen, and B_2H_6 or PH_3) or by sputtering from the doped targets in a mixture of argon and hydrogen. Depending on the deposition parameters, the doped films were either totally amorphous or partially crystallized [3–5].

The investigated solar cell structures are either single or tandem pin structures. The p and n layers were fabricated either by sputtering from the intrinsic target and employing gas phase doping or by sputtering from the doped targets. In both cases the p and n layers were deposited under conditions to be either amorphous or partially crystallized. To minimize cross contamination effects between the layers it was found necessary to scrupulously clean the deposition chamber in between. Since contamination of the chamber by boron [6] was found to be far more severe than contamination by phosphorus [7] the most efficient cells were fabricated in the configuration: stainless steel/nip/ITO.

The standard process of depositing such a device involved the following steps. First 200–400 Å of the n layer was deposited. Then the sample was covered with a shutter and a hydrogen rich discharge was ignited for a period of 3–6 h. A pure argon discharge could attain the same results but for a longer period of time. The length of cleaning time was found to also depend on the temperature of the walls of the apparatus. We speculate that the mechanism of plasma cleaning of the phosphorus species is partly due to physical sputtering and partly due to chemical sputtering (conversion of the elemental phosphorus into volatile hydrides, which progressively are pumped out of the deposition system). After this step, the intrinsic film was deposited to a total thickness of approximately 0.5 μm. Next, 150 Å of p layer was deposited. Between the intrinsic and p layers the deposition was also interrupted for approximately 10–20 min for the adjustment of the deposition parameters appropriate for the p layer. The ITO layer was deposited also by sputtering in another sputtering system. The thickness of this layer was adjusted to be approximately 700 Å. The sheet resistance of such layers was found to depend sensitively on the previous history of the ITO target. The best films were found to have a sheet resistance of about 50–100 Ω/□.

The films were characterized by employing a number of structural probes (X-ray diffraction, SEM, index of refraction) and by measuring their optical, transport and recombination properties. The devices were evaluated by studying their I–V characteristics and the collection efficiency spectra.

3. Experimental results and discussion

3.1. Properties of intrinsic films

The photovoltaic properties of the intrinsic films were found to depend on structural and compositional inhomogeneities, amount of hydrogen in the films, trace impurity doping and compensation. Some of these results have been discussed elsewhere [6–13]. In this paper we give only a brief summary of these results and emphasize the most salient features.

There are two types of structural inhomogeneities in amorphous silicon. One is associated with the columnar growth [14] and the other with microvoids of ~ 10 Å in diameter [15]. In amorphous silicon produced by sputtering the structural inhomogeneities due to columnar growth can be controlled by charged particle bombardment [2,16]. Such charged particles include Ar^+, H^+ and Si^+ (ionized by the Penning process) and secondary electrons. We have argued previously [16] that moderate secondary electron bombardment is preferable, since Ar^+ ion bombardment could lead to the formation of microvoids. The deposition parameters which control such charged particle bombardment are the total pressure of the sputtering gas [16], the target voltage [17], and the substrate bias [16]. It was found that the films with the best structural homogeneity are produced at low total pressure ($Ar + H_2 < 15$ mTorr), moderate substrate positive bias (30–50 V) and moderate target bias voltage (-800 to -1500 V). Substrate temperatures of between 400 and

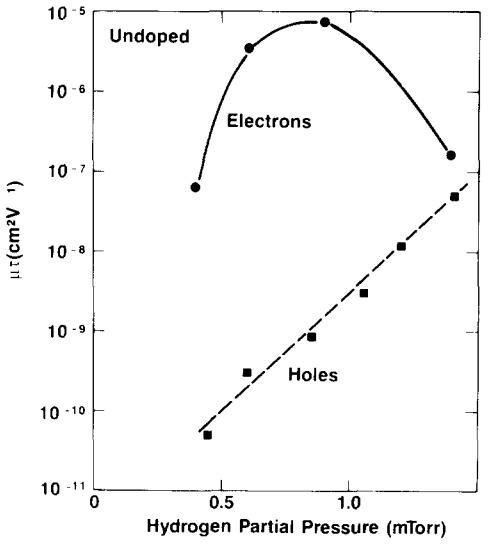

Fig. 1. ($\mu\tau$) Products for electrons and holes for intrinsic films vs partial pressure of hydrogen.

500°C could also have the same effect [2]. However, at such high temperature, hydrogen evolution leads to material with large number of silicon dangling bonds.

Compositional inhomogeneities in hydrogenated amorphous silicon are related to hydrogen bonded in different local environments. We reported earlier [2,16] that the compositional inhomogeneities of sputtered material can be improved under moderate electron bombardment. We have also shown that compositional inhomogeneities do not affect the density of silicon dangling bonds but they do affect the optical properties of the films [2].

The opto-electronic properties of films with the best structural and compositional homogeneity depend sensitively on the amount of hydrogen in the films [8–10]. To illustrate this point we show in fig. 1 the dependence of mobility-lifetime ($\mu\tau$) product for both electrons and holes for a series of films produced with the partial pressure of hydrogen as the parameter. The ($\mu\tau$) product for electrons was calculated from photoconductivity measurements utilizing volume absorbed light. All values were normalized to the same generation rate (1×10^{19} carriers/(cm^3 s)). The ($\mu\tau$) product for holes was calculated from collection efficiency measurements of Pt-Schottky barrier structures [9].

The monotonic increase of ($\mu\tau$) for holes is related to monotonic decrease of silicon dangling bonds with hydrogen content [8]. The variation of ($\mu\tau$) for electrons requires a more detailed analysis and is discussed elsewhere [18]. It is important to note that the material with the best photoconductivity is not optimum for photovoltaic applications. The best photovoltaic material is the intrinsic material, which has the same ($\mu\tau$) for both the electrons and holes (10^{-7} cm^2/V).

The effect of hydrogen on the photovoltaic properties of the intrinsic films is illustrated in fig. 2. These data show the J_{sc} and V_{oc} of Pt-Schottky barrier structures as a function of partial pressure of hydrogen in the discharge. Over the investigated

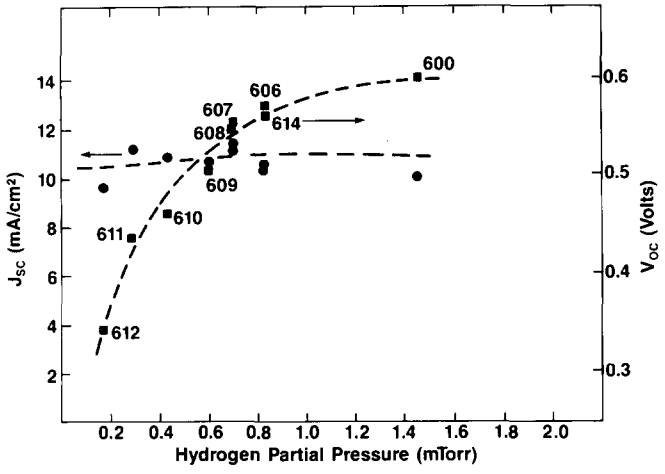

Fig. 2. J_{sc} and V_{oc} of Pt-Schottky barrier structures vs the hydrogen pressure in the discharge.

range the V_{oc} increases from 0.35 to 0.6 V while the J_{sc} remains in the range of 10 to 12 mA/cm^2. The increase of the V_{oc} is related to the increase of the energy gap of the material from 1.6 to 1.85 eV [10]. The insensitivity of the J_{sc} with the hydrogen content can be understood in a simple model [9] in which the collection efficiency is given by:

$$Y(\lambda) = 1 - \exp(-X_c\alpha(\lambda)), \tag{1}$$

where X_c is the collection width and $\alpha(\lambda)$ is the optical absorption coefficient. The quantity X_c improves with hydrogen content [9], but correspondingly the optical absorption decreases. The insensitivity of the J_{sc} suggests that the product $X_c\alpha(\lambda)$ is almost constant for the investigated hydrogen range. The data of fig. 2 suggest that the films with the larger gap have the potential to lead to photovoltaic devices with the maximum V_{oc} and no significant degradation in J_{sc}.

The effects of phosphorus and boron impurities on the photovoltaic properties of the intrinsic films were investigated by studying ni–Pt-Schottky barrier structures whose i layer was contaminated intentionally with small amount of B_2H_6, PH_3 or both [6,7]. The conclusions from these studies are the following. Small amounts of contamination by phosphorus (1–10 ppm) dopes the material n-type with corresponding decrease of ($\mu\tau$) product for holes. It is therefore necessary to scrupulously clean the deposition chamber between n and i layers during the fabrication of substrate/nip devices. The tolerance to contamination by boron of the intrinsic films depends on the position of the equilibrium Fermi level in the intrinsic films. When the equilibrium Fermi level is exactly in the middle of the gap, as in the best material, even less than 0.5 ppm of B dopes the material p-type [6]. Intrinsic films grown with only 0.05 ppm of B_2H_6 in the discharge were found to have the best photovoltaic properties. Presumably such a small amount of B is needed to compensate residual donors in our films.

3.2. Properties of doped films

We discuss first doped films produced by gas phase doping. Such films were produced either in amorphous or microcrystalline forms. The critical deposition parameters for the transition from the one regime to the other have been discussed in other papers [3–5]. In the present paper we discuss only the transport and optical properties of these two classes of materials, since these properties are related to photovoltaic application. The amorphous films were deposited at 325°C with $H_2 + Ar = 5$m Torr ($H_2/Ar = 0.2$) and 0.2 at% of B_2H_6 in the discharge. The microcrystalline films were also deposited at 325°C with $H_2 + Ar = 40$ mTorr ($H_2/Ar = 10$) and 0.2 at% of B_2H_6 or PH_3 in the discharge respectively.

Fig. 3 shows the temperature dependence of the conductivity for two microcrystalline films doped p-type (sample #475) and n-type (sample #440) and one

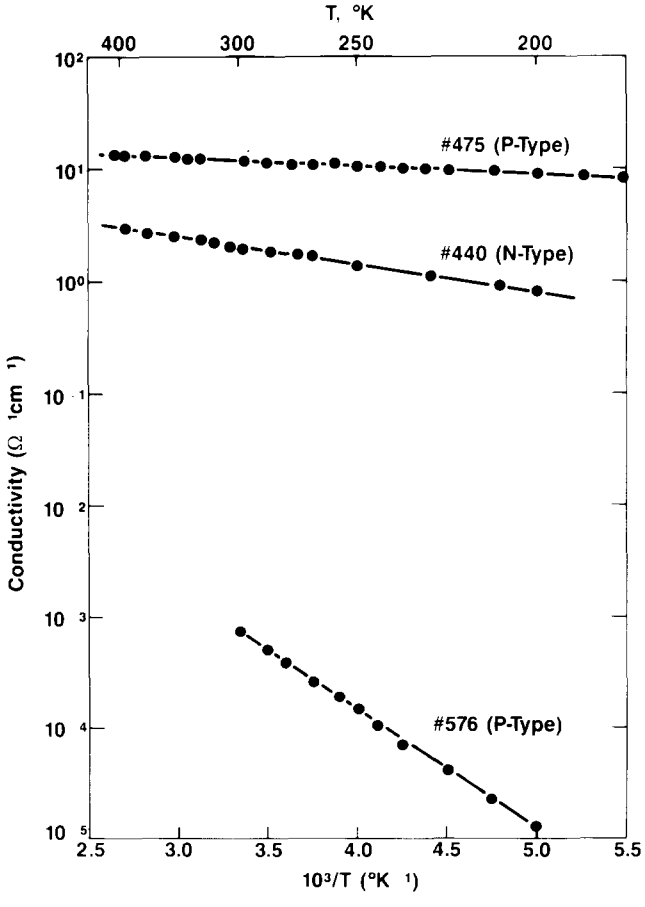

Fig. 3. Dark conductivity vs $1/T$ for two microcrystalline films doped p-type and n-type (sample #475 and #440) and one amorphous film doped p-type (sample #576).

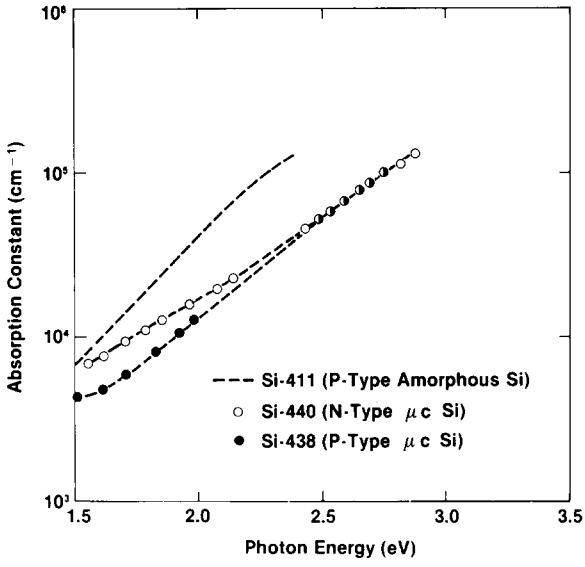

Fig. 4. Optical absorption constant vs photon energy for amorphous and microcrystalline silicon doped films.

amorphous film doped p-type (sample #576). The conductivity of the microcrystalline films is several orders of magnitude higher than that of the amorphous film. Also the lack of significant temperature dependence in the microcrystalline films suggest that these materials are degenerate semiconductors.

Fig. 4 shows the optical absorption constant as a function of photon energy for one amorphous p-type film (sample #411) and two microcrystalline films (samples #438 and #440). Note that the microcrystalline films are far more transparent in the visible part of the spectrum than the amorphous film.

Doping from heavily doped targets was found to be less efficient than doping by gas phase. Both the amorphous and microcrystalline films produced from the doped targets were found to be approximately two orders of magnitude less conductive than corresponding films produced by gas phase doping. We speculate that the source for it is depletion of dopant atoms from the surface of the target through the formation of volatile hydrides.

3.3. Solar cell structures

Solar cell structures were fabricated on polished stainless steel substrates having dimensions 2.5″ × 2.5″. Because of the severity of contamination by boron, the highest efficiency devices were deposited in the configurations: S/nip/ITO/grid or SS/nip–nip/ITO/grid. The ITO layer was deposited through a metal mask in order to define 14 areas of 1 cm^2. The metal grid (Au or Ag) was also deposited through a metal mask. A representative sample is shown in fig. 5. The equivalent performance

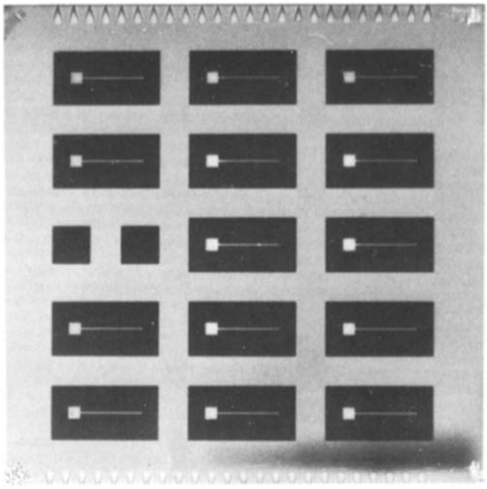

Fig. 5. Representative solar cell structure having the configuration SS/nip/ITO/Au or SS/nip-nip/ITO/Au. The substrate area is 2.5″×2.5″ and each device has an area of 1 cm^2.

of all 14 devices is suggesting that the uniformity of the different layers is excellent.

The highest efficiency devices were deposited with microcrystalline p and n layers because of their reduced optical absorption in the visible spectral region and their increased conductivity. The intrinsic layer in such devices contains approximately 0.05 ppm of boron. Fig. 6 shows the $I-V$ characteristics of a device with the highest observed efficiency. The J_{sc} and V_{oc} of this device are identical to those of similar devices (SS/pin(μC)/ITO), fabricated by the method of glow discharge decomposi-

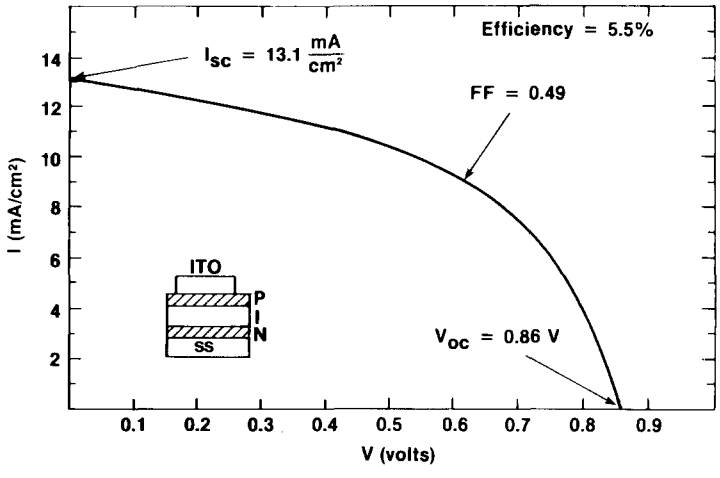

Fig. 6. $I-V$ characteristics of a sputtered SS/nip/ITO solar cell structure.

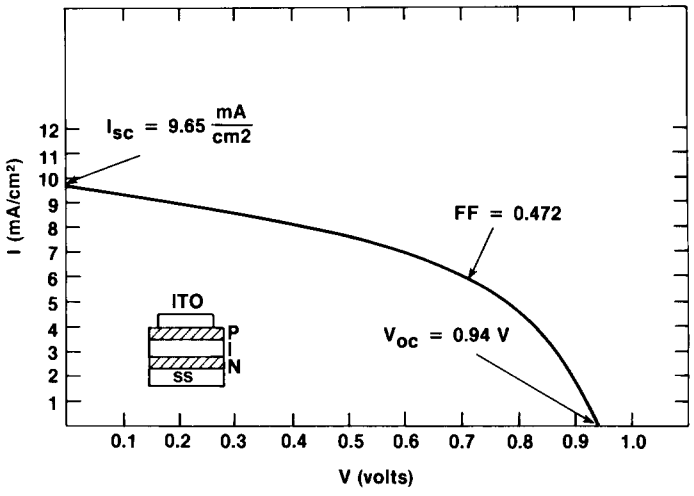

Fig. 7. $I-V$ characteristics of an identical solar cell structure as that shown in fig. 6 but with thicker p-contact.

tion of silane [19]. The glow discharge device is illuminated from the n layer, which is microcrystalline.

The open circuit voltage of the sputtered devices can be increased by changing the energy gap of the intrinsic layer. In addition, we find that V_{oc} depends on the thickness of the p layer. Fig. 7 shows the $I-V$ characteristics of a SS/nip/ITO solar cell structure fabricated under identical conditions as the device shown in fig. 6 but with 250 Å of p layer instead of 150 Å. This device has the highest V_{oc} reported in the literature. The reduction of J_{sc} in this device is related to additional absorption loss in the p layer. The increase of V_{oc} with the thickness of the p layer is attributed to reduction in recombination at the ITO/p interface.

The short circuit current can be improved by implementing light trapping techniques or using p-type silicon carbide layers, which are far more transparent than the microcrystalline p-type silicon films. As an example, we show in fig. 8 how the incorporation of back reflective contacts can improve the red portion of the collection efficiency. The two devices have the configurations indicated in the insert of the figure. The TiO_2 layer, approximately 30 Å thick, acts to prevent diffusion of silver into the amorphous silicon. The highest efficiency glow discharge devices have the configuration: glass/SnO_2/p$^-$(SiC)in/Ag. Light trapping in such devices is implemented by both texturing the SnO_2 layer and providing a reflective back contact [20].

The poor FF of the sputtered devices is attributed to the degradation of interfaces due to the prolonged sputter cleaning between the layers. We therefore propose that fabrication of these devices in three dedicated chambers would lead to devices with improved FF.

Devices were also fabricated in tandem configurations. Fig. 9 shows the $I-V$ characteristics of a tandem solar cell structure, having the configuration indicated in

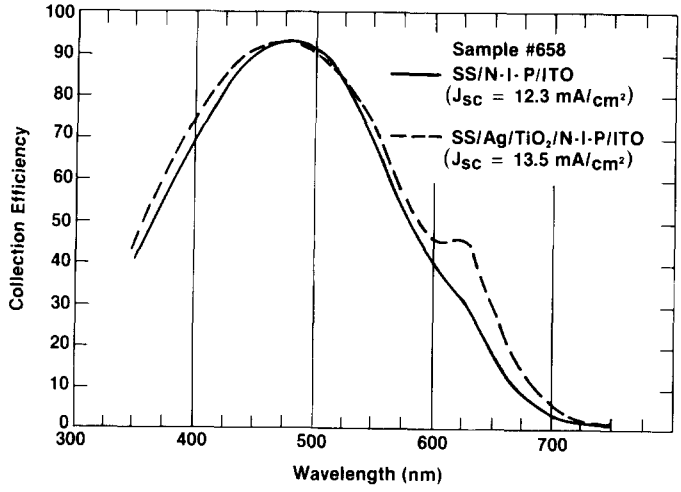

Fig. 8. The effect of substrate reflectivity on the spectral dependence of the collection efficiency of sputtered solar cells.

the insert of the figure. The p and n layers were microcrystalline, each with a thickness of 150 Å, and the two i-layers were amorphous, each with a thickness of 3000 Å. This $I-V$ characteristic suggests that the p and n microcrystalline layers are sufficiently degenerate so that a tunneling current between the two pin cells encounters negligible impedance. The value of the voltage is twice that of a single pin device. The current in the example is relatively small because the two pin cells have not been matched for maximum current. However, these initial results suggest that high efficiency tandem cells can be fabricated by the sputtering method if either

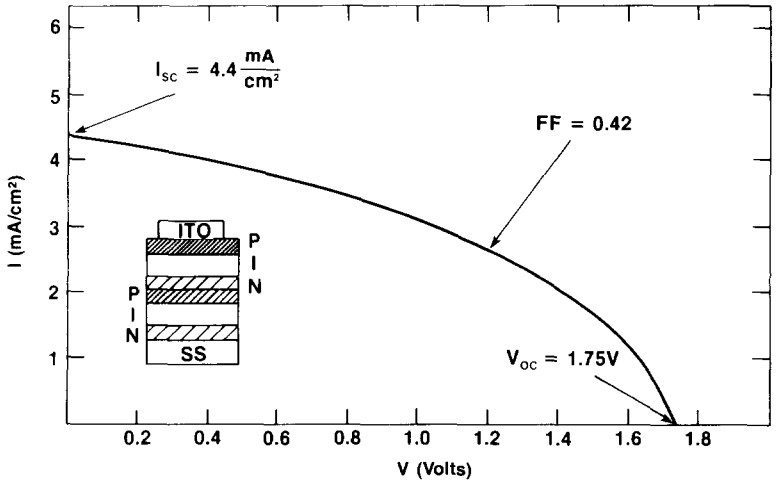

Fig. 9. $I-V$ characteristics of a sputtered tandem solar cell.

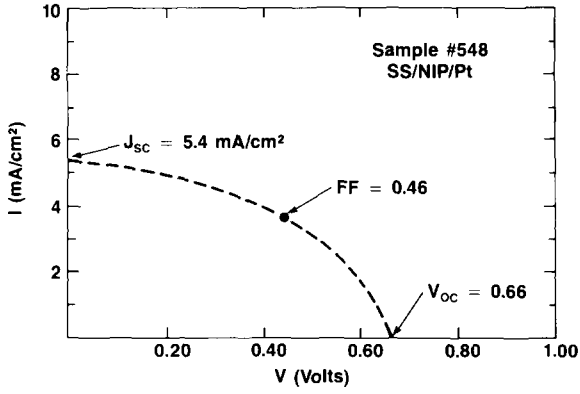

Fig. 10. $I-V$ characteristics of a SS/nip/Pt solar cell structure with the n and p layers deposited from doped targets.

a smaller gap intrinsic material is used in the back solar cells, or the thickness of the two intrinsic layers is properly tailored.

The devices discussed so far have been fabricated by doping the p and n layers through gas phase doping. Fig. 10 shows the $I-V$ characteristics of a solar cell structure, having the configuration indicated in the insert of the figure, with microcrystalline p and n layers deposited from the B- and P-doped targets. The p and n layers in this device are microcrystalline, produced by sputtering from the doped targets at a mixture of $Ar + H_2 = 40$ m Torr ($H_2/Ar = 10$). The intrinsic layer was produced under similar conditions as in the previous devices. During the deposition of this device it was also found necessary to interrupt the discharge between the n and i depositions and sputter-clean the chamber for residual phosphorus contamination. This finding agrees with our hypothesis that the surfaces of the doped targets are depleted of dopant atoms by a hydrogen transport mechanism. The smaller V_{oc} in this device is related to the poorer doping of the p and n layers as explained earlier. The smaller J_{sc} is related to absorption at the Pt-contact. Further optimization of this process is required.

4. Conclusions

We have investigated the photovoltaic properties of hydrogenated amorphous silicon films produced by reactive RF diode sputtering. The study covered the properties of intrinsic films, doped films, and various solar cell device structures.

The photovoltaic properties of the intrinsic films depend sensitively on structural and compositional inhomogeneities, amount of hydrogen in the films, trace impurity doping and compensation. In particular we find that the best films are those with approximately 10–20 at% hydrogen and approximately 0.05 ppm of B impurities. These films are intrinsic and have ($\mu\tau$) products for both electrons and holes of 10^{-7} cm^2 V^{-1}. The optical gap of these films is 1.8 eV.

Doped films have been produced both by gas phase and by sputtering from heavily doped targets. The first process was found to be more efficient. Microcrys-

talline films produced by both processes have optical and transport properties, which are more suitable for photovoltaic applications.

The combination of the best intrinsic and doped films led to the fabrication of pin solar cell structures with efficiencies of 5.5%. The efficiency is limited by the poor FF which was attributed to interface degradation. We suggested ways to improve the V_{oc}, J_{sc} and FF. Finally, unoptimized tandem solar cell structures and pin solar cells with the doped layers deposited from doped targets have been presented.

The results presented in this paper suggest that the photovoltaic properties of the sputtered material are equivalent to those of material produced by the method of glow discharge decomposition of silane.

Acknowledgements

The author is indebted to P. Maruska, A. Rose, T. Tiedje, C. Wronski for a number of technical discussions and to R. Friedman and M. Hicks for technical assistance. The work was partially supported by the U.S. Department of Energy through a Solar Energy Research Institute Contract (Contract #ZB-3-02166-01).

References

[1] F.J. Krampas, in: Semiconductors and Semimetals, vol. 21A, ed. J.I. Pankove (Academic Press, New York, 1984) ch. 8.
[2] T.D. Moustakas, in: Semiconductors and Semimetals, vol. 21A, ed. J.I. Pankove (Academic Press, New York, 1984) ch. 4.
[3] T.D. Moustakas, D.A. Weitz, E.B. Prestridge and R. Friedman, in: Plasma Synthesis and Etching of Electronic Materials Mat. Res. Soc. Symp. Proc. vol. 38 (1985) p 401.
[4] T.D. Moustakas, H.P. Maruska and R. Friedman, J. Appl. Phys. 58 (1985) 983.
[5] T.D. Moustakas, in: Tetrahedrally Bonded Amorphous Semiconductors, eds. D. Adler and H. Fritzsche (Plenum, 1985) p. 39.
[6] T.D. Moustakas, H.P. Maruska, R. Friedman and M. Hicks, Appl. Phys. Lett. 43 (1983) 368.
[7] T.D. Moustakas, R. Friedman and B.R. Weinberger, Appl. Phys. Lett. 40 (1982) 587.
[8] T. Tiedje, T.D. Moustakas and J.M. Cebulka, Phys. Rev. B23 (1981) 5634.
[9] T.D. Moustakas, C.R. Wronski and T. Tiedje, Appl. Phys. Lett. 39 (1981) 721.
[10] D.L. Morel and T.D. Moustakas, Appl. Phys. Lett. 39 (1981) 612.
[11] T.D. Moustakas, in: Photovoltaics for Solar Energy Applications II, ed. D. Adler, Proc. SPIE 407 (1983) 56.
[12] T.D. Moustakas, Proc. 5th EC Photovoltaic Conf. (Reidel, Dordrecht, 1983) pp. 698–706.
[13] T.D. Moustakas, Proc. Symp. on Materials and New Processing Technologies for Photovoltaics, vol. 83-11 (The Electrochemical Society, 1983) p. 291.
[14] J.C. Knights and R.A. Lujan, Appl. Phys. Lett. 35 (1979) 244.
[15] W. Paul, G.A.N. Connell and R.J. Temkin, Adv. Phys. 22 (1973) 529.
[16] T.D. Moustakas, Solar Energy Mater. 8 (1982) 187.
[17] T.D. Moustakas and H.P. Maruska, Appl. Phys. Lett. 43 (1983) 1037.
[18] T.D. Moustakas and C.R. Wronski, to be published in Appl. Phys. Lett.
[19] Y. Uchida, T. Ichimura, M. Veno and H. Haruki, Jpn. J. Appl. Phys. 21 (1982) L586.
[20] A. Catalano, R.V. D'Aiello, J. Dresner, B. Faughnan, A. Firester, J. Kane, H. Schade, Z.E. Smith, G. Swartz and A. Traino, IEEE Photovoltaic Spec. Conf. 16 (1982) 1421.